September 1984

Rare-earth—gallium—iron glasses. I. Magnetic ordering and hysteresis in alloys based on Gd, Tb, and Er

S.G. Cornelison
University of Nebraska - Lincoln

David J. Sellmyer
University of Nebraska-Lincoln, dsellmyer@unl.edu

Rare-earth—gallium—iron glasses. I. Magnetic ordering and hysteresis in alloys based on Gd, Tb, and Er

S. G. Cornelison* and D. J. Sellmyer
Behlen Laboratory of Physics, University of Nebraska, Lincoln, Nebraska 68588-0111
(Received 28 October 1983)

Results of magnetic measurements are presented on the new metallic glass systems $(R_{80}Ga_{20})_{100-x}Fe_x$ and $(R_{80}Ga_{20})_{90}B_{10}$, where R denotes the heavy rare earths Gd, Tb, and Er, for $x=10$, 20, and 30, respectively. High-field magnetization (to 80 kOe) and ac and dc susceptibility measurements were made from 1.4 to 300 K. The Gd-Fe glasses are simple ferrimagnets with opposing Gd and Fe moments. The Gd-B glass exhibits two apparent transitions (paramagnetic—ferromagnetic—like, and ferromagnetic spin-glass) as the temperature is lowered. As Fe is added, the low-temperature transition disappears. The data can be understood in terms of Sherrington-Kirkpatrick—type models for the phase diagram with competing ferromagnetic and spin-glass order. In the Tb and Er glasses a strong local random anisotropy prevents saturation of the magnetization in high fields, and the ac susceptibility shows sharp peaks indicating speromagnetic (spin-glass-like) order. In high fields the moment approaches that expected for a hemisphere of randomly oriented spins ($\frac{1}{2}gJ$/spin), so that an asperomagnetic structure is produced by the applied field. For small values of x (10 and 20), the Tb and Er glasses exhibit coercive force, H_c, and hysteresis characteristics consistent with coherent-rotation processes. However, for large Fe concentrations ($x=30$), the ac susceptibility peaks are considerably smeared, suggesting increased chemical short-range order and increased heterogeneity. The observed increase of H_c in these alloys seems to be consistent with the theory of Paul, although the choice of parameters is not well defined. The temperature dependence of H_c for the $x=30$ alloys indicates that domain-wall motion or nucleation processes appear to dominate magnetization reversal.

I. INTRODUCTION

Metallic glasses based on $3d$ transition metals are often soft ferromagnets which exhibit small coercivities and are easily saturated in low applied magnetic fields. The fundamental reasons for this behavior in concentrated $3d$ alloys are the absence of a large spin-orbit interaction in light elements and the "quenching" of the orbital angular momentum. Since the $3d$ spins are effectively decoupled from the lattice because of this effect, the energetic barriers to spin alignment with an applied field are small as is necessary for soft ferromagnets. Metallic glasses based on the rare earths, however, usually exhibit quite different behavior.[1] Since the $4f$ electronic wave functions responsible for the presence of a magnetic moment on rare-earth ions are buried relatively deeply within the ion, they retain much of their atomiclike character and there is little or no quenching of the orbital angular momentum.[2] This is especially true of the heavy rare earths, but the light rare earths may exhibit a more complex magnetic behavior.[3–6] Thus in rare-earth-based alloys (except Gd, La, and Lu) we expect a large spin-orbit interaction through which the spins may strongly couple to the local environment. In order to explain results of magnetic measurements on metallic glasses which show large curvature in the high-field magnetization, reduced spontaneous magnetization and often large coercive forces, Harris *et al.*[1,7] presented a theory in which a local uniaxial anisotropy with random orientation was assumed at each rare-earth site.

In the local-random-anisotropy model of Harris, Pliscke, and Zuckermann (HPZ) it was assumed that the uniaxial anisotropy was constant in magnitude but varying in direction. The HPZ Hamiltonian is[7]

$$H=-\tfrac{1}{2}\mathcal{J}\sum_{i,j}[\vec{J}(i)\cdot\vec{J}(j)]-D\sum_i(\hat{n}_i\cdot J_z^{(i)})^2-\mu H\sum_i J_z(i)\ , \tag{1}$$

where $\mathcal{J}$ is the exchange, μ is the magnetic moment, $\hat{n}_i$ is the local (random) easy axis, and D is the single-ion anisotropy. This was solved in the molecular-field approximation. The ground state obtained by Harris *et al.* is asperomagnetic for $\mathcal{J}>0$ with a "spontaneous magnetization," M_0, of $\frac{1}{2}gJ$/spin. If $\mathcal{J}$ is taken to be negative, a speromagnetic (or spin-glass-like) state is obtained in which the spins are distributed randomly in direction and $M_0=0$. However, more recent calculations by other workers using different techniques have predicted the true ground state to be speromagnetic or spin-glass-like for $\mathcal{J}>0$.[8,9] Also, more recently, Harris[10] has concluded that an asperomagnetic state, but with 25% of the spins reversed to the lower hemisphere, is the true ground state. Using another approach Callen *et al.*[11] have proposed a microdomain model which predicts that at intermediate ratios of anisotropy to exchange, coherent regions will exist with spins directed along a regional easy axis. This result was in agreement with predictions of Chi and Alben[12] and Alben *et al.*,[13] in which the ground state was

described as consisting of domains, i.e., a "polydomain" model.

In the present work an attempt will be made to interpret experimental results within the framework of some of the above theories. Because of the crystal anisotropy present in rare-earth alloys, many promising permanent magnet materials such as RA_5 and the R_2A_{17} compounds are being extensively studied with R a rare earth and A=Co, Fe, or Ni.[14–18] Recently, however, there have been theoretical predictions which suggest the heterogeneity of the magnetic material may play an important role in determining the magnetic hardness.[19,20] Thus some rare-earth metallic glasses, which may be magnetically quite heterogeneous because of random fluctuations or a phase separation, may be expected to be magnetically hard. In the light of these predictions and some initial results on amorphous $(Pr_{80}Ga_{20})_{80}Fe_{20}$,[21,22] we extended our study to the systems $(R_{80}Ga_{20})_{100-x}Fe_x$ where $0<x<30$, and R=Gd, Tb, and Er. In this paper we will present results of x-ray diffraction, dc and ac magnetic susceptibility, and high-field magnetization measurements. An attempt will be made to interpret the magnetic hardness of these materials in terms of the presence of site-of-site fluctuations in the magnetic properties of these glasses.

II. EXPERIMENTAL METHODS

Alloys of $(R_{80}Ga_{20})_{100-x}Fe_x$ for $x \leq 30$ and R=Gb, Tb, and Er were prepared by arc melting under argon. The purities of the elements used were at least 99.9%. Buttons of polycrystalline material were then melted in a modified arc-melting furnace whereupon they were rapidly quenched to obtain amorphous foils of thickness about 50 μm. X-ray diffraction measurements employing a Si(Li) detector were made to ensure that the samples were amorphous. It was found that some crystalline lines were present in alloys containing no Fe, so that 10 at. % boron was added to these samples to produce the amorphous state. Figure 1 shows a typical Mo $K\alpha$ diffraction pattern for $(Gd_{80}Ga_{20})_{90}B_{10}$. The liquidlike structure is evident.

ac susceptibility measurements were performed between 4.2 and 300 K. This apparatus employed a balanced pair of coils, a driving field of about 0.3 Oe, and was operated at a frequency of 280 Hz. Standard phase-sensitive detection techniques, a probe slowly lowered into a helium bath, and a computer-controlled data-acquisition system were employed. Faraday susceptibility measurements and high-field magnetization studies were performed between 4.2 and 300 K with systems that have been described previously.[23,24]

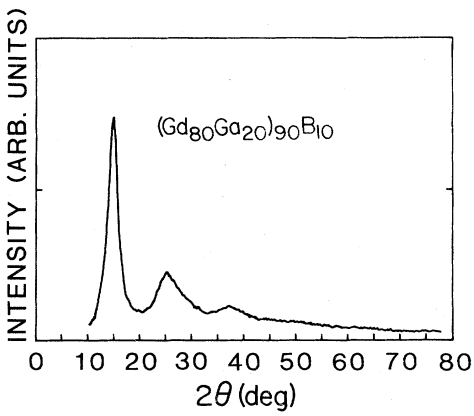

FIG. 1. Mo $K\alpha$ x-ray diffractogram on amorphous $(Gd_{80}Ga_{20})_{90}B_{10}$.

III. ASPECTS OF DATA ANALYSIS

In this paper two methods are employed to obtain the spontaneous magnetization M_0 and the uniaxial anisotropy constant K. K is related to D by $K=nD$, where n is the spin density. The first method is based on the usual form for the empirical law of approach to ferromagnetic saturation:[25]

$$M=M_0\left[1-\frac{A_1}{H}-\frac{A_2}{H^2}\cdots\right]+\chi_H H\ , \tag{2}$$

where M_0 is the spontaneous magnetization and χ_H is the high-field susceptibility. The coefficient A_2 is determined by the anisotropy K, as well as by magnetoelastic stresses, and is taken to be[26]

$$A_2=\tfrac{4}{15}(K^2/M_0)\ . \tag{3}$$

The term A_1 is determined by plastic deformations, nonmagnetic inclusions,[27] dislocation dipoles,[28] or other inhomogeneities within the samples. Fairly good fits are obtained at high fields with $A_1=0$, but in the intermediate-field regions the H^{-1} term is shown to be important.

The second method for estimating the anisotropy constant is called the magnetization-area method. Here, K is given by[29]

$$\int_{M_R}^{M_0} H\,dM=\tfrac{2}{3}K\ , \tag{4}$$

where M_R is the remanent magnetization and the integral corresponds to the area to the left of the $M(H)$ curve as the field is decreased from the saturation value to zero. There are several limitations to this technique which should be mentioned. The most obvious problem is the lack of observable saturation at high fields with the available 80-kOe field. Many of the alloys studied still may have considerable curvature at up to 200 kOe. Thus this technique will obviously give too *small* a value in those cases. Also, at low applied fields, various processes such as domain-wall diffusion, etc., occur, and the spins do not rotate directly against forces of anisotropy. However, by extrapolating χ_H, which often decreases nearly linearly as H is increased, to obtain an estimate of the saturation field, a more reasonable estimate of K can be made. It is interesting that in nearly every case this method gives values of K in reasonable agreement with results of the fits to the law of approach to saturation.

IV. RESULTS AND DISCUSSION OF GENERAL MAGNETIC PROPERTIES

A. Gd-based glasses

Results of ac susceptibility measurements on the $(Gd_{80}Ga_{20})_{100-x}Fe_x$ for $x=10$ and 20 are presented in

Fig. 2. Also shown are data for $(Gd_{80}Ga_{20})_{90}B_{10}$. As mentioned above, the boron was required to stabilize the glassy phase in this case. Hereafter, the boron-containing glass will be denoted as the $x=0$ glass for convenience. In each case, samples of equal mass, which were rectangular strips measuring about 1 mm$\times$4 mm$\times$50 μm, were placed with their long axes parallel to the applied ac magnetic field. The measured ac susceptibility is given by

$$\chi_{ac}=\frac{dM}{dH_a}=\frac{dM}{d(H+NM)}\ , \tag{5}$$

where the applied field is $H_a=H+NM$ with N the demagnetization factor. In the limit that the true susceptibility, $\chi=dM/dH$, diverges, $\chi_{ac}\rightarrow N^{-1}$. Thus for a ferromagnetic transition at T_c, χ_{ac} becomes a constant, and if there is a sharp flattening of the measured susceptibility, a reasonably accurate measurement of T_c can be obtained. Such apparent ferromagnetic transitions are seen in Fig. 2 at 122, 172, and 219 K, for the $x=0$, 10, and 20 samples, respectively. Since deviations of χ_{max} $(=N^{-1})$ were less than 10% for different samples, the demagnetization factors are fairly well known.

The increase in T_c with Fe concentration is understandable in terms of a mean-field model for which T_c is proportional to $\mathcal{J}_0$, the average exchange.[1] On the other hand, the low-temperature drop in χ_{ac} for the $x=0$ sample is less easily explained. The two possibilities are (a) a "reentrant" or ferromagnetic—spin-glass transition[30] at about $T_{fg}=50$ K, or (b) the magnetic hardening of a multidomain ferromagnet as the result of the pinning of domain walls below 50 K. Figure 3 shows χ_{ac} for the $x=0$ sample for the fields parallel and perpendicular to the plane of the sample strips. χ_{max} scales approximately as the demagnetization coefficient. In addition, the inset shows how the coercive force H_c increases below about 25 K. On the basis of these data alone it is not possible to conclude with certainty that either the "double-transition" or "hysteretic ferromagnet" hypothesis is correct. However, there are several factors that make the ferromagnetic—spin-glass transition explanation likely. The first is that the Sherrington-Kirkpatrick[31] phase diagram suggests that in a system with an average ferromagnetic exchange of magnitude $\mathcal{J}_0$ and with exchange fluctuations of average magnitude $\Delta\mathcal{J}$, there will be such double transitions when $\Delta\mathcal{J}/\mathcal{J}_0\simeq 1$. We have discovered[32] in the related system $Gd_xLa_{72-x}Ga_{18}B_{10}$ that a complete phase diagram can be determined with paramagnetic, ferromagnetic, and spin-glass regions; there is an apparent multicritical point (MCP) at $x=67$. The concentration dependence of these data suggests that there are, in fact, considerable exchange fluctuations so that one is near a MCP in the $(Gd_{80}Ga_{20})_{100-x}Fe_x$ system. Moreover, the increase in $\mathcal{J}_0$ as x increases would move one *away* from the MCP in the phase diagram and remove the ferromagnetic—spin-glass transition—just as was observed.

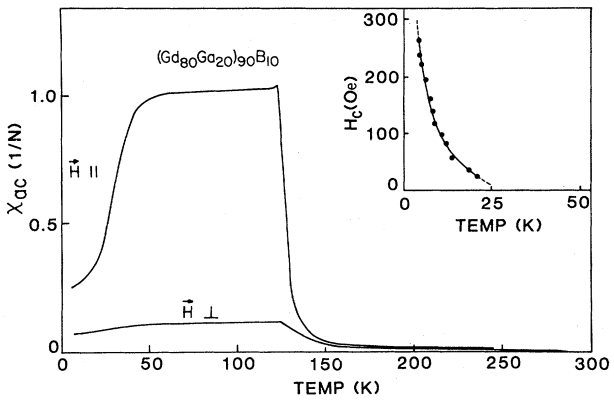

FIG. 3. ac measurements on $(Gd_{80}Ga_{20})_{90}B_{10}$ with the sample parallel to field orientation and perpendicular to field orientation. Inset shows coercive field (H_c) against temperature.

Figure 4 shows high-field magnetization of all three alloys at 4.2 K in units of emu/g. The values obtained for the spontaneous magnetization M_0 by extrapolation of

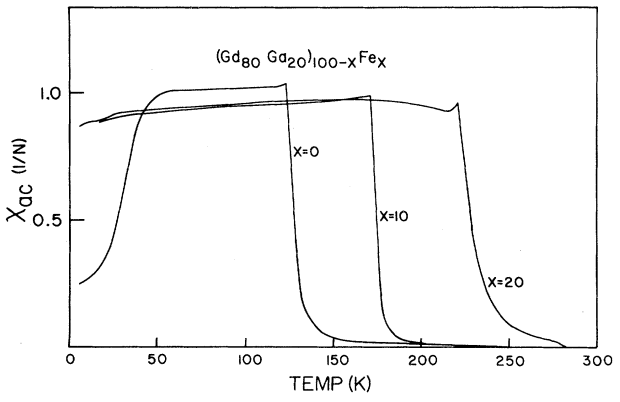

FIG. 2. ac susceptibility measurements on Gd-based glasses. The glass marked $x=0$ is $(Gd_{80}Ga_{20})_{90}B_{10}$. The scale on the vertical axis is chosen by averaging several measurements on infinite-susceptibility glasses whose maximum value of χ_{ac} is $1/N$. Thus the value of N varies by less than 10% for these samples. This is expected to be the case for all other samples discussed in this paper.

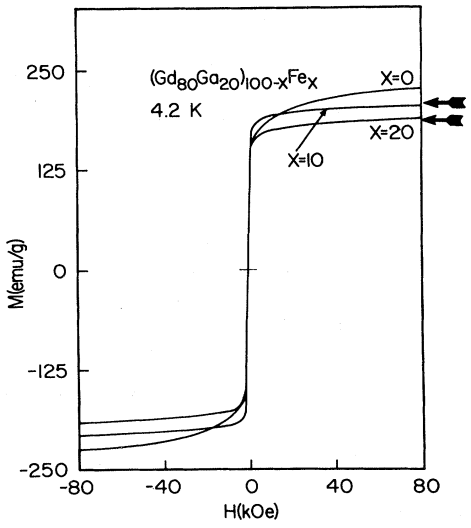

FIG. 4. High-field magnetization measurements on Gd-based glasses. Thick arrows indicate complete spin alignment (see test).

high-field data to $H=0$ are 220, 200, and 178 emu/g for the $x=0$, 10, and 20 alloys, respectively. Corresponding values obtained for M_0 from fits to Eq. (2) are 220.9, 200.7, and 177.5 emu/g. The spontaneous moments calculated for ferromagnetism for the glass containing no iron and for antiparallel alignment of Gd and Fe spins in the other glasses are indicated by thick arrows in the figure (assuming $gJ=7\mu_B$ for Gd and $2.2\mu_B$ for Fe). Clearly, the Fe-containing glasses are ferrimagnetic as expected for Gd alloys with magnetic transition-metal solutes.

In Fig. 4 it is interesting that the $x=0$ glass is magnetically harder than the samples containing Fe. The magnetization-area method of estimating K [Eq. (4)] leads to $K\simeq 1.5\times 10^7$ erg/cm^3, a rather large value for an S-state ion with little or no spin-orbit coupling. Table I lists the anisotropy constants, as well as other parameters obtained from fits to Eqs. (2)–(4). It should be noted that the K value for the $x=20$ sample is about 4 times *smaller* than that for the $x=0$ sample. In view of the above discussion of the likelihood of this being a system with competing ferromagnetic and spin-glass order, we suggest that the relatively large K value for the $(Gd_{80}Ga_{20})_{90}B_{10}$ glass is due to some admixture of antiferromagnetic coupling in the exchange distribution, and thus is *not* due to local random anisotropy caused by electric field gradients operating on Gd ions containing some orbital angular momentum in their wave functions. The increase of the average exchange ($\mathcal{J}_0$) as Fe is added and the consequent decrease in the measured K support this model.

B. Tb-based glasses

ac susceptibility measurements made on the Tb alloys $(Tb_{80}Ga_{20})_{100-x}Fe_x$ for $x=10$, 20, and 30 are shown in Fig. 5, as well as data for $(Tb_{80}Ga_{20})_{90}B_{10}$. The addition of 10 at. % B was required for this alloy to stabilize glass formation. Hereafter, this glass $[(Tb_{80}Ga_{20})_{90}B_{10}]$ will be called the Tb $x=0$ glass for convenience. The scale is normalized to the scale of the previous Gd alloys, and all of the alloys have the same mass and geometry and are oriented the same as discussed before. The $x=0$ sample has a peak at 63 K, while the others show peaks at 87, 134, and 180 K for $x=10$, 20, and 30, respectively. While the other alloys have a single peak which increases as Fe is added, the 30-at. % Fe alloy has a dramatic drop in χ_{max} and a second broad peak develops at lower temperatures. The inset in Fig. 5 shows results of measurements on the $x=0$ and samples in which the field was applied in the parallel and the perpendicular orientations. For the 20-at. % alloy, the ration $\chi_{\perp}^{max}/\chi_{\parallel}^{max}$ was about 12%, but for the alloy containing no iron, the ratio was about 37%. Figure 6 shows the results of dc susceptibility measurements on the $x=0$ and 20 glasses using the Faraday technique; similar data were obtained on the $x=10$ and 30 glasses. Open circles represent data obtained after cooling in zero applied field and solid circles represent data obtained after cooling in an applied field of about 700 Oe. All data were taken as the temperature was raised. The two curves meet at a temperature (T_F) where the spin-freezing processes apparently begin. The peaks in ac susceptibility are indicated by vertical arrows. The ac measurements in low fields are apparently a more precise measure of the onset of spin-freezing processes.

Examples of hysteresis loops for $x=20$ and 30 are shown in Fig. 7. Sharp discontinuities are observed, particularly at 2.2 K for $x=30$, where a large number of apparent domain walls moving in cascade lead to the magnetization reversals observed. Results of analysis of magnetization loops using the magnetization-area method and the law of approach to saturation are given in Table I. In each case that the magnetization failed to approach the value for complete alignment even in fields of 80 kOe, a large high-field susceptibility was observed and large intrinsic coercivities developed at low temperatures.

The above susceptibility and magnetization data for the

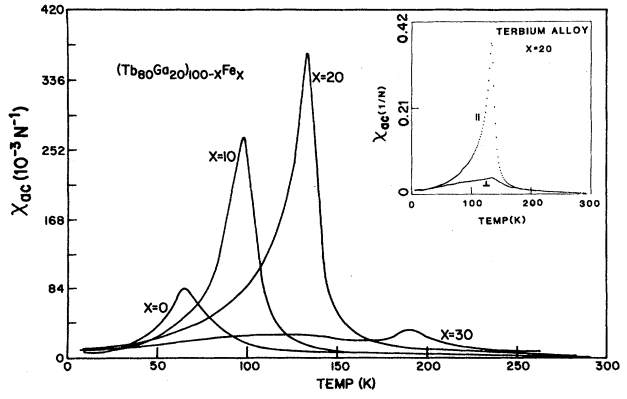

FIG. 5. ac susceptibility for Tb-based glasses. The $x=0$ glass is $(Tb_{80}Ga_{20})_{90}B_{10}$. The inset shows the results of measurements in both parallel and perpendicular to the applied magnetic field. The large difference in χ_{ac} for the two orientations suggests the value of χ_{ac} is controlled by demagnetization effects indicating a large susceptibility at χ_{max} (see text).

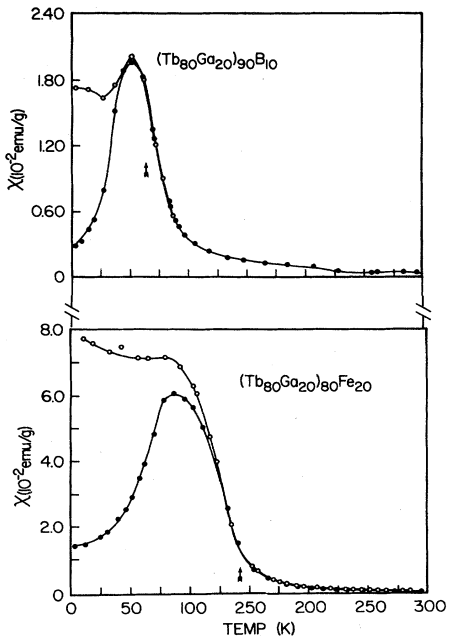

FIG. 6. dc susceptibility of $(Tb_{80}Ga_{20})_{90}B_{10}$ and $(Tb_{80}Ga_{20})_{90}B_{20}$. The vertical arrows indicate spin-freezing temperatures obtained by ac measurements.

TABLE I. Results of analysis of magnetization loops using the magnetization-area method and the law of approach to saturation.

	M_0[a] (emu/g)	$\langle \frac{1}{2}gJ \rangle$[b] (emu/g)	μ_{Fe}[c] (emu/g)	K[d] (10^7 erg/cm^3)	M_R'	$H_c(0)$[e] (kOe)	$H_c^{th}(0)$[f] (kOe)	$H_c^{th}(0)$[g] (kOe)	χ_H (10^{-6} emu/g)
$(Gd_{80}Ga_{20})_{90}B_{10}$	220.9	110.5	0	1.5 (2.5)		≈0.70	0.7	0.77	91
$(Gd_{80}Ga_{20})_{90}Fe_{10}$	200.7	107	9.4	(1.10)					57
$(Gd_{80}Ga_{20})_{80}Fe_{20}$	177.5	101.5	20.0	(0.6)		≈0.15			127
$(Tb_{80}Ga_{20})_{90}B_{10}$	148	140	0	3.5 (3.6)	0.52	≈44	40	UV[b]	373
$(Tb_{80}Ga_{20})_{90}Fe_{10}$	137	136	9.3	2.34 (2.28)	0.72	40	40	UV[h]	156
$(Tb_{80}Ga_{20})_{80}Fe_{20}$	147.5	129	19.8	1.67 (1.87)	0.83	40	43	61	253
$(Tb_{80}Ga_{20})_{70}Fe_{30}$	137.1	121	31.9	1.50 (1.90)	0.77	≈40	45	52.4	275
$(Er_{80}Ga_{20})_{90}B_{10}$	140.1	135	0	(3.1) 4.2	0.17				390
$(Er_{80}Ga_{20})_{80}Fe_{10}$	130.5	130.5	8.9	(2.6) 2.7	0.25				310
$(Er_{80}Ga_{20})_{80}Fe_{20}$	144	124.3	19.0	(2.8) 2.4	0.46	≈6.0	6.5		230
$(Er_{80}Ga_{20})_{70}Fe_{30}$	137.9	119.0	30.7	(2.8)	0.51	≈10	9.0	16.5	192

[a] M_0 is from law of approach to saturation fits.
[b] This value is one-half the aligned-moment value for the rare-earth ions (assuming free-ion moments).
[c] This is the aligned-moment value for the Fe ions, assuming 2.2 μ_B/Fe.
[d] This is the anisotropy from magnetization-area method and law of approach to saturation measurements, the latter in parentheses.
[e] This is the extrapolated (to $T=0$) value of H_c from experimental data.
[f] $H_c(0)$ obtained from the fit to the theory of Gaunt.
[g] $H_c(0)$ obtained from the fit to the theory of Egami.
[h] UV denotes unphysical values that were obtained ($> 10^6$ Oe).

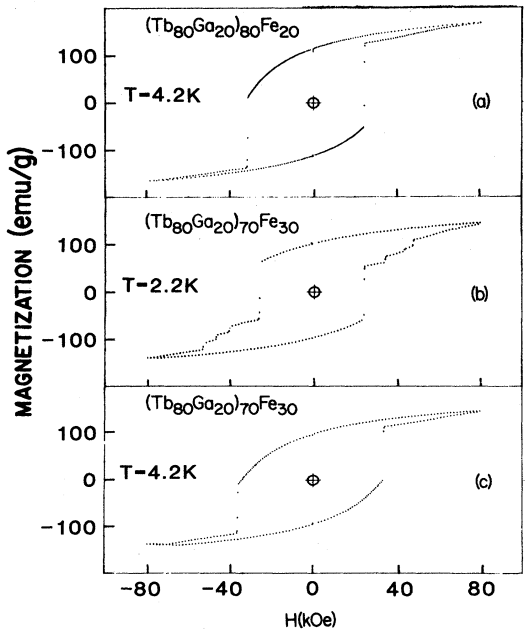

FIG. 7. High-field magnetization of the $x=20$ and 30 glasses. These jumps in $M(H)$ may be indications of microdomains (see text).

Tb glasses lead to the following picture of their magnetic structure. The sharp χ_{ac} peaks and field-cooling effects seen in the dc susceptibility indicate speromagnetic transitions into a random spin-glasslike structure. As Fe is added the magnitude of χ_{ac}^{max} increases but does not approach N^{-1}. For $x=20$, $\chi_{\perp}^{max}/\chi_{||}^{max}=0.12$, which is similar to the ratio expected on the basis of $N_{||}/N_{\perp}$ (also see Fig. 3). Thus for this sample the Fe has driven the system towards a ferromagneticlike state where χ diverges, but has not yet reached such a state. The large local random anisotropy produces the scattered spin arrangement, in agreement with the general theoretical results, which preclude a state with long-range magnetic order in dimensions less than four, in the presence of random magnetic anisotropy (RMA).[33] In the case of the $x=30$ sample, the ac susceptibility peak is weakened and broadened, suggesting perhaps a system with significant chemical short-range order (CSRO) magnetic clusters, and a smeared magnetic transition.

C. Erbium-based glasses

Figure 8 shows results of ac susceptibility measurements on Er-based glasses of composition $(Er_{80}Ga_{20})_{100-x}Fe_x$ where $x=0$, 10, 20, and 30. For the $x=0$ glass, 15 at. % boron is added to stabilize the glass.

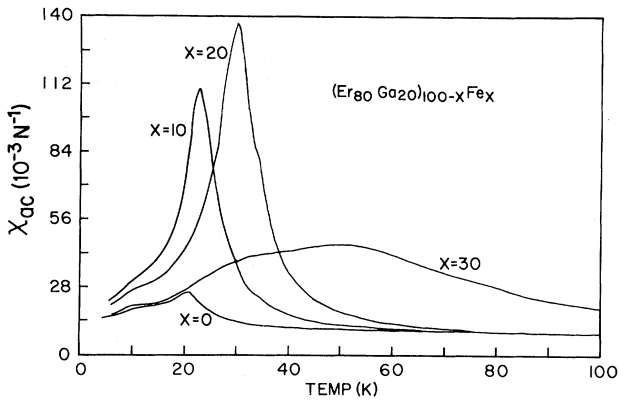

FIG. 8. ac measurements on Er glasses. The $x=0$ glass is $(Er_{80}Ga_{20})_{85}B_{15}$. Note how the value of χ_{max} is reduced below Tb glasses but that similarities between corresponding glasses are pronounced.

This glass will be called the Er $x=0$ glass hereafter for convenience. The scale on the susceptibility axis is in units of N^{-1}, where N is an average demagnetizing factor for these samples as determined from infinite-susceptibility Gd samples. Full scale is about 0.45 emu/g Oe. ac susceptibility peaks, apparently at spin-freezing temperatures, occur at 20, 23, 31, and about 50 K for $x=0$, 10, 20, and 30, respectively. The strong reduction in χ^{max} observed in these glasses indicates that they are not ferromagnetic and suggests a speromagnetic ground state. The reduction in susceptibility for the $x=30$ glass is quite similar in character to that for the Tb $x=30$ glass. A magnetic character quite different from that of the $x=0$, 10, or 20 alloys is indicated and, again, a cluster glass is suggested with significant CSRO.

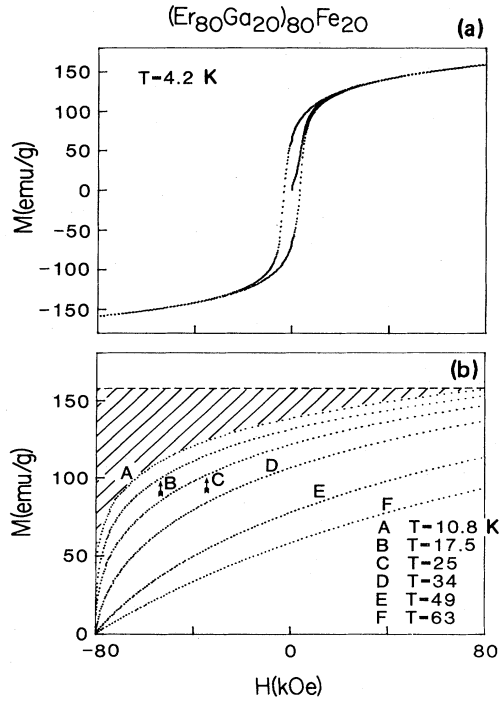

FIG. 9. High-field magnetization for Er-based glasses.

High-field—magnetization data of Er glasses were fit to the law of approach to saturation to determine spontaneous moments, anisotropy constants, and the high-field susceptibility χ_H. The M_0 values obtained (see Table I) were in agreement with asperomagnetic order in high fields for the $x=0$ glass, while alloys containing Fe, as with Tb glasses, gave M_0 values somewhat larger than expected for asperomagnetic order and with Fe spins reversed. It is interesting that none of the magnetization loops at low temperatures displayed giant discontinuities as did Tb-based glasses. In addition, the coercive fields were greatly reduced from corresponding Tb glasses. This can be seen from Fig. 9(a) which shows a 4.2-K hysteresis loop for the $x=20$ glass. Figure 9(b) shows field sweeps at different temperatures. The hatched area to the left of the 10.8-K sweep can be used to measure the anisotropy constant by the magnetization-area method. Interestingly, the coercive field at 4.2 K for the $x=30$ glass is larger from that for the case of $x=0$, 10, or 20. The same was true for the $x=30$ glass of Tb. These observations show the systematic similarity between Er and corresponding Tb glasses. The differences in the two systems seem to be *quantitative* ones reflecting difference exchange and local RMA strengths.

V. MAGNETIC HYSTERESIS IN Tb- AND Er-BASED GLASSES

The preceding glasses, except those based on Gd, all exhibit magnetic hardness at low temperatures. This is due largely to the anisotropy, K, which tends to compete against exchange forces in an attempt to align spins along the local easy-magnetization axis. For an array of single-domain particles with uniaxial anisotropy at random directions, Stoner and Wohlfarth[34] predicted magnetic hysteresis as is shown in Fig. 10(a).[35] Figure 10(b) shows a low-temperature loop for $(Tb_{80}Ga_{20})_{90}B_{10}$. The character of this loop is similar to that for noninteracting single-domain particles as shown in Fig. 10(a). Since then there have been several theories predicting giant intrinsic magnetic hardness in amorphous magnets. A theory by Bishop and Lewis,[36] which models domain walls by solitons, predicts domain-wall pinning to occur when the domain-wall width becomes a few lattice spacings. Chi and Alben[12] predict an abrupt increase in coercivity when $D/\mathcal{J}\approx 5$ for amorphous uniaxial magnets, while Patterson *et al.*,[37] using a local—mean-field-approximation technique, predict a similar increase at $D/\mathcal{J}=7$. Ferrer *et al.*,[38] using Monte Carlo techniques, have considered the case of $\mathcal{J}<0$ (antiferromagnetic coupling) and have found that $H_c\approx 0.95D$ when $D/|\mathcal{J}|\gtrsim 2.5$. Using the molecular-field approximation, Callen *et al.*[11] have predicted the existence of "microdomains" in large anisotropy amorphous magnets. These are regions where local magnetization tends to point along a dominant easy-magnetization axis and which interact with one another by the molecular field λM.

In the following sections we compare our results with several theories of magnetic hardness. These include microscopic models relevant to $T=0$ and also models intended to explain the temperature dependence of the coercivity.

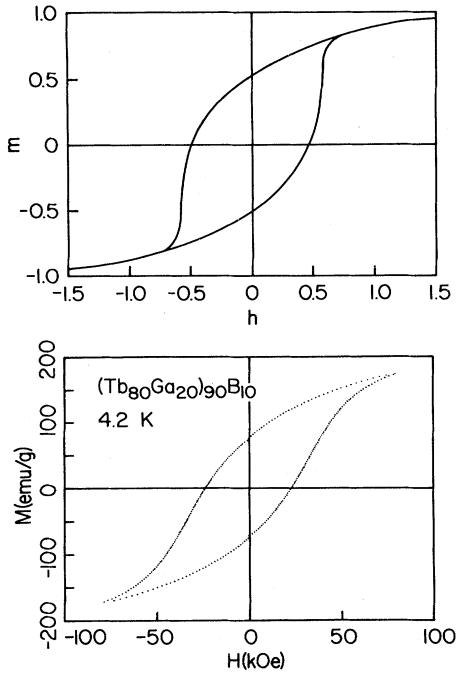

FIG. 10. Hysteresis loop at $T=0$ for system of noninteracting single-domain particles with uniaxial anisotropy (top). Hysteresis loop for $(Tb_{80}Ga_{20})_{90}B_{10}$ at 4.2 K (bottom).

A. Zero-temperature microscopic models

The microdomain theory of Callen *et al.*[11] predicts for positive λ the onset of a coercive field at $d\sim 2.5$, where $d=D/\lambda n\mu^2$ with D being the single-ion anisotropy, λ being the molecular-field constant, and μ being the moment. Figure 11(a) shows the reduced remanence M_R' versus d for $d>0$. In the case of ferromagnetic microdomain interactions, d is small and M_R' is large (approaching 1) but for large d, M_R' approaches 0.5, the Stoner-Wohlfarth value. Also predicted are discontinuous jumps in the initial magnetization as shown in Fig. 11(b). Figure 11(c) shows the predicted coercive force against d in the Callen *et al.* model. This is contrasted with a saturation of H_c at $D/\mathcal{J}>5$ as predicted by Chi and Alben.[12] Figures 12 and 13 show initial magnetization curves (taken at intermediate sweep rates) for some Tb and Er alloys, respectively, at 4.2 K. The Fe-containing Tb alloys show discontinuous jumps at about 30 kOe, which occur at higher fields if the sweep rate is lowered. Fe-containing Er alloys show increases at much smaller fields, and no large discontinuities appear, but small jumps are observed as the hysteresis loop is traversed. The large discontinuities observed in Tb alloys (see Fig. 7) are typical of other Tb alloys such as $TbFe_2$ (Ref. 39) and $Tb_{75}Au_{25}$ (Ref. 29).

These discontinuities have been explained as a thermomagnetic effect in which heat released a local magnetization reversal activates nearby regions to reverse, etc., until thermal equilibrium has been reached.[40] The jumps observed involve volumes of about 10^{-5} cm^3 (Er glasses) to 10^{-3} cm^3 (Tb glasses) as determined by assuming these regions of spin reversal to be "saturated" to the "spontaneous" moment obtained by the law of approach to saturation.

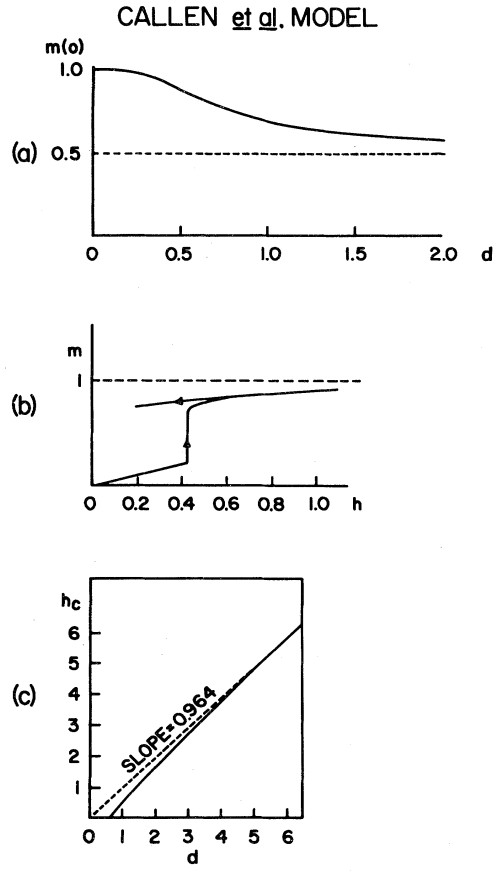

FIG. 11. Predictions of the Callen *et al.* model for interacting single-domain particles with random anisotropy at $T=0$. The value d is the ratio of the anisotropy to the interaction strength (exchange). In (a) the reduced remanence $m(0)\equiv M_R'$ in text is plotted against d. For strongly interacting systems d is small and $m(0)$ is nearly 1. (b) shows predicted jumps in the initial magnetization curve and (c) shows the reduced coercivity vs d. h_c should be small when the reduced remanence $m(0)$ is large. Figures are taken from Ref. 11.

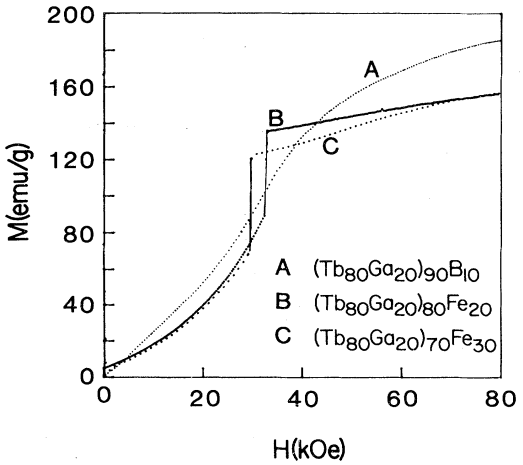

FIG. 12. Initial magnetization curves at 4.2 K for Tb-based glasses.

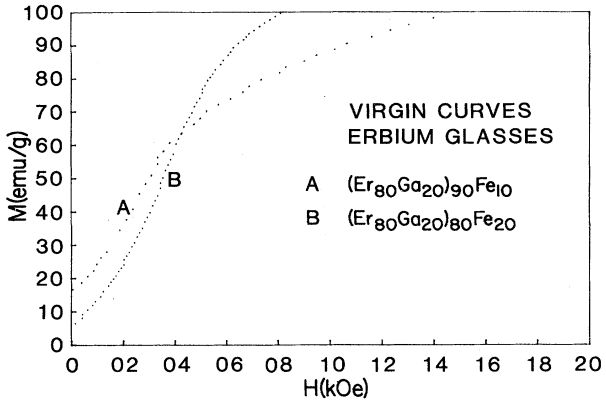

FIG. 13. Initial magnetization curves at 4.2 K for Er-based glasses.

The virgin curves of the Er alloys suggest a spin-flop process. This follows because of the relatively low fields at which there are inflection points in $M(H)$ (2—4 kOe), and by analogy with antiferromagnetic intermetallic compounds such as $ErGa_2$ ($T_N=7.5$ K, where spin-flop fields of about 6 and 18 kOe are observed).[41] Because of expected disorder and exchange fluctuations in the Er glass, one would not expect a sharp spin-flop field. This type of behavior has been predicted by Ferrer *et al.* and Bhattacharjee and Coqblin for the case of a random antiferromagnet spin flopping to a random ferromagnet.[38] The presence of antiferromagnetic interactions in Er alloys is supported both by the greatly reduced M_R' which is *below* 0.5, and by the much reduced ac susceptibility peaks observed in these alloys as was shown in Fig. 8. In the Er alloys (Fig. 13) it appears that the critical spin-flop field *decreases* as Fe content decreases (d increasing). This is consistent with predictions of Ferrer *et al.*[38] in a quantum-mechanical mean-field approximation, but is the reverse of results of a Monte-Carlo calculation and of the classical mean-field approximation of Callen *et al.*[11] However, the presence of a spontaneous moment in these glasses may complicate this interpretation. The case for Tb glasses (Fig. 12) is different. Here, the $x=30$ glass shows a "jump" at a lower field than the $x=20$ glass. Using a technique outlined in a previous paper[29] and values of M_R', K, and M_0 obtained by the law of approach to saturation or the magnetization-area method, we obtain, for $(Tb_{80}Ga_{20})_{90}B_{10}$, $\lambda \lesssim 5$. This suggests, within the model, a very weakly interacting spin system and leads to $H_c \approx 32$ kOe, a value of the order of the extrapolated experimental value of ≈ 44 kOe. However, M_R' for Fe-containing alloys increases as the Fe content increases, suggesting the presence of interactions which should *decrease* d and therefore H_c (since $0.964D=H_c$). For $(Tb_{80}Ga_{20})_{70}Fe_{30}$, $M_R'=0.77$, which leads to $H_c \approx 0.4K/M_0 \approx 7.5$ kOe, a value greatly reduced from the expected $H_c(0)$ (Table I) of 40 kOe. Coercive forces predicted by Ferrer *et al.*[38] for random antiferromagnetic systems suggest values reduced from the ferromagnetic case with equal $D/|\mathcal{J}|$. Following the procedure of Ferrer *et al.*, a value of $H_c(0)=18.8$ kOe is obtained for $(Er_{80}Ga_{20})_{90}B_{10}$, while 14.5 kOe is obtained for $(Er_{80}Ga_{20})_{70}Fe_{30}$. Extrapolated values (Table I) are ~ 6 and 10 kOe, respectively. Thus values of $H_c(0)$ do not decrease in Er alloys with increasing Fe concentration as is predicted.

Obviously, the above comparison of experimental data to theory requires the use of values obtained from experiment of M_0, K, and χ_H. Since Fe is expected to align antiparallel with rare-earth ions in these alloys and Er alloys have speromagnetic (or possibly spin-glass) ground states, the high-field data may give extrapolations on the basis of which only qualitative agreement with the theory could be expected.

B. Anisotropy and exchange fluctuation model: $T=0$

It has been suggested by several authors that it is the presence of *fluctuations* in the strength of anisotropy and exchange that can lead to a large intrinsic magnetic hardness in anisotropic materials.[20,42] Recently, Friedberg and Paul[19] have presented a domain-wall—pinning model which has been successful in predicting the coercive force (H_c) in many materials. Using this theory, which predicts pinning at "fluctuation" sites, and which Paul has applied to amorphous materials,[43] we obtain the following form relating H_c to other magnetic parameters:

$$H_c=\frac{2}{\sqrt{27}}\frac{K_1 W}{M_1\delta_1}\left[\frac{J_1}{J_2}-\frac{K_2}{K_1}\right], \tag{6}$$

where K_1, J_1, δ_1, and M_1 are the anisotropy, exchange, domain-wall width parameter, and magnetization of magnetic region 1, and K_2, and J_2 are similar parameters of region 2, the defect region ; W is the width of region 2.

Although this theory has been developed for ferromagnetic materials with *planar* defects parallel to domain walls, Paul suggests that these may be "breakaway regions" where part of the domain wall is parallel to part of the defect during the wall motion and Eq. (6) is obeyed. In order to compare the theory to realistic materials, reasonable values for the fluctuation term are chosen, viz.,

$$(A_1/A_2-K_2/K_1)\approx 0.2\ , \tag{7}$$

with $A_1/A_2 \approx 1.1$ and $K_2/K_1 \approx 0.9$, so that fluctuations are considered to be relatively small. Also, W is chosen to be 7.5 Å, a reasonable grain-boundary width; these assumptions lead to

$$H_c \cong 0.57K_1/M_1\delta_1 \text{ Å}\ ,\quad \delta_1=(A_1/K_1)^{1/2}\ , \tag{8}$$

which gives good agreement when applied to many materials (including amorphous $GdCo_4$). If we use $K_1=1.5\times 10^7$ erg/cm^3 obtained for $(Gd_{80}Ga_{20})_{90}B_{10}$ and $M_1=1540$ emu/cm^3 we obtain $H_c \approx 5.55\times 10^3$ Å Oe/δ_1. By using

$$A_1=3k_BT_c/Za\ , \tag{9}$$

where $Z \cong 12$ near neighbors and $a \approx 3$ Å, a value of 550 Oe is obtained for H_c in this alloy which is close to (≈ 700 Oe) the experimentally extrapolated value. A similar treatment on $(Gd_{80}Ga_{20})_{80}Fe_{20}$ with $K \approx 0.6\times 10^7$ erg/cm^3 and $M=1390$ emu/cm^3 gives $H_c=137$ Oe compared to the experimental values of ≈ 150 Oe. The same method leads to $H_c=4$ kOe for $(Tb_{80}Ga_{20})_{90}B_{10}$, an order

of magnitude too small, while smaller values are found for other Tb alloys. Also, the theory predicts values of 9.4 and 2 kOe for $(Er_{80}Ga_{20})_{90}B_{10}$ and $(Er_{80}Ga_{20})_{70}Fe_{30}$, respectively. However, the latter extrapolated experimental value is greater than 10 kOe. These results, which are worse for increasing Fe content, may suggest the presence of greater fluctuations than this theory can take into account. (The above theory, derived using a perturbation technique, is valid only for materials with small fluctuations.)

In amorphous materials containing magnetic transition metals in a $4f$ or $5f$ host matrix, it is expected that hybridization of $3d$ levels can lead to reduced or vanishing moments on $3d$ sites whose local environment is deficient in $3d$ neighbors.[44,45] Thus the random nature of metallic glasses may lead to a distribution of moments at Fe sites and greatly increase the magnetic fluctuations of a material. Recently, Paul[46] has extended and improved the above theory to take into account *large* fluctuations in the site-to-site magnetic properties of materials. By making the assumption that the sample on the average has two types of magnetic regions, and estimating the parameters F and E (in Paul's figures) from expected magnetic constants within these regions, a maximum possible H_c for the material can be estimated. The ac susceptibility of $(Tb_{80}Ga_{20})_{70}Fe_{30}$ shows greatly reduced and broadened peaks (see Fig. 5). This suggests the possibility of relatively large heterogeneity within this sample. By assuming this sample has Fe-rich and Tb-rich regions (defect and host region), and using parameter values obtained from $(Tb_{80}Ga_{20})_{70}Fe_{30}$ and $(Tb_{80}Ga_{20})_{90}B_{10}$, respectively, an estimate of $H_c^{\max}$ can be made. By assuming $T_{c2}\approx 200$ K and $T_{c1}=100$ K and values $K_1\approx 3.5\times 10^7$ erg/cm^3, $K_2\approx 1.0\times 10^7$ erg/cm^3, $M_2=900$ emu/cm^3, and $M_1=110$ emu/cm^3, then an $H_c^{\max}$ of from 33 kOe to about 50 kOe is predicted (using generated graphs in Paul's paper). The experimental extrapolated value is about 40 kOe. Obviously, values obtained in this way are dependent on a choice of input parameters and unless accurate microscopic information is available, they should be considered only as order-of-magnitude results. It is not even certain that domain-wall motions are a dominant mechanism of spin reversal in highly anisotropic random alloys. $(Tb_{80}Ga_{20})_{90}B_{10}$, for example, seems to resemble a system of loosely interacting particles in which a coherent-rotation mechanism is active, as seen in Fig. 10. It is interesting that the above theory, in the limit of a nonmagnetic defect, predicts

$$H_c=2K_1/M_1\ , \tag{10}$$

the maximum expected H_c for coherent rotation for a uniaxial particle in the Stoner-Wolfarth theory.[34] Thus the theory may be expected to have applicability, even in the limit of single-domain-particle coherent rotations.

C. Temperature dependence of coercive field in a coherent rotation model

The properties most important to magnetic hardness are the intrinsic coercive force H_c, and the magnetization M. Well below the ordering temperature where M is nearly saturated, it is the coercive force which may determine the magnetic "hardness" of many materials. It has been shown that single-domain particles may spontaneously reverse their magnetization direction if the height of the barrier to coherent rotation is $\approx k_BT$. Bean and Livingston[47] have found (for a single-domain particle with the reverse field along the axis) the temperature dependence of H_c to be

$$H_c=H_0[1-5(k_BT/KV)^{1/2}]\ , \tag{11}$$

where H_0 is the coercive force at $T=0$, V is the volume, and K is the uniaxial anisotropy density. More recently, several authors have improved this calculation by including an *array* of noninteracting uniaxial particles with axes randomly oriented to H_a.[48–50].

The proposed microdomain theory of Callen, Cullen, and Liu, which modified the Stoner-Wohlfarth coherent-rotation process at $T=0$ by an exchange-enhanced effective field,[11] has been extended to finite temperatures by Gaunt.[51] Using a load-line technique and assuming that d $(=D/\lambda M_0^2)$ and V are constant over the temperature range, he obtained a reasonable fit at low temperatures to the results of Rhyne *et al.* for amorphous $TbFe_2$.[39] With the use of these techniques for different values of d, fits were obtained on Tb alloys as shown in Fig. 14. For $(Tb_{80}Ga_{20})_{90}B_{10}$ the fit was obtained with a domain volume $V=2180$ Å^3, $d=1$, and $H_c^0=20$ kOe. The dashed line indicates the fit for a system of noninteracting spins as in Eq. (12) with $K=4.9\times 10^7$ erg/cm^3 and $V=1950$ Å^3. The fits are good at low temperature but fail in all cases above ≈ 20 K. Gaunt, who observed similar behavior in $TbFe_2$ fits, suggests that a range of values of λ in the sample may cause this behavior. For the noninteracting case the theory suggests that a model in which V decreases as T increases would better fit these experimental data. Figure 15 shows similar fits to some

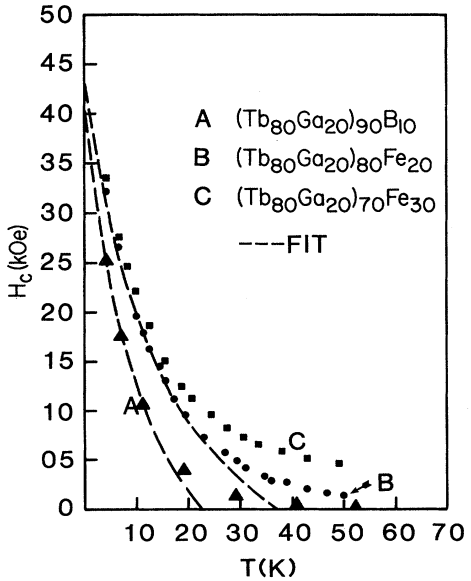

FIG. 14. Experimental fits to Gaunt's theory. The dashed lines represent the best fit to the data for samples A and B. Note that the data deviate from the theory above about 15 K (sample A) and 25 K (sample B).

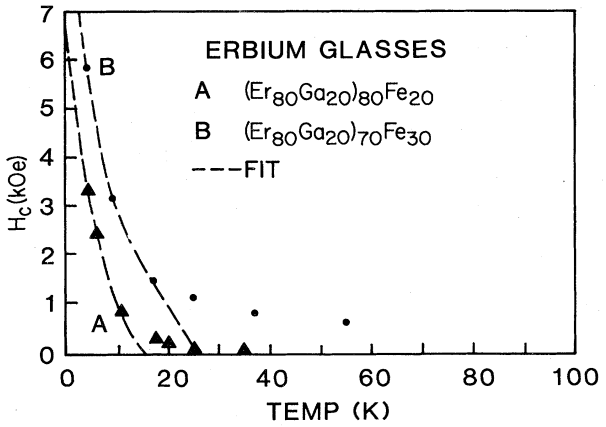

FIG. 15. Experimental fits to Gaunt's theory of the thermal variation of H_c for the Er-based glasses. The dashed lines represent the fit to theory.

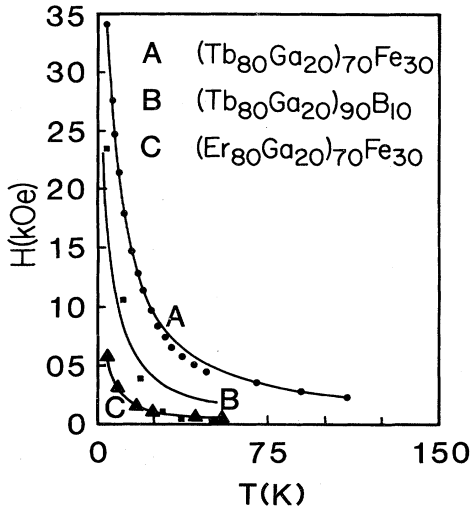

FIG. 16. Experimental fits to Egami's theory of the thermal variation of H_c for some Tb- and Er-based alloys. The dashed lines represent the fit to theory. Note the poorer fit in B. A coherent rotation model fits data on $(Tb_{80}Ga_{20})_{90}B_{10}$ better.

Er alloys. The behavior is seen to parallel that for Tb alloys except in the $x=0$ and 10 alloys that show a peak in H_c at lower temperatures. These dropoffs at low T could be a manifestation of a domain-wall tunneling process predicted by Egami.[52]

D. Temperature dependence of intrinsic coercive field in a domain-wall diffusion model

If domain walls are assumed within these materials, then the intrinsic magnetic hardness could be due to internal energy barriers to domain-wall propagation or nucleation. The probability for domain-wall motion against barriers of energy height E is given by

$$\tau^{-1}=Ce^{-E/k_BT}, \tag{12}$$

where $C\approx\exp(25)$ Hz.[53] If we take $\tau\approx 1$ sec,

$$25k_BT=E\ . \tag{13}$$

Egami[52] has shown that (for homogeneous nucleation processes)

$$E=\frac{16\langle S^2\rangle \mathcal{J}}{n}\frac{H_c}{H}G\left[\frac{H}{H_c}\right], \tag{14}$$

which may be approximated by[54]

$$25k_BT=\frac{16\langle S^2\rangle \mathcal{J}}{n}\frac{H_c}{H}\left[1-\left[\frac{H}{H_c}\right]^2\right] \tag{15}$$

and fitted by

$$H_c=H_0\{[1+(V_TT)^2]^{1/2}-V_TT\}\ , \tag{16}$$

where H_0=coercivity at $T=0$, and $V_T=(25\text{ K})n/\mathcal{J}\langle S^2\rangle$ with $\mathcal{J}\langle S^2\rangle$ equal to the exchange strength and n equal to the width of domain wall in lattice spacings. Least-squares fits of experimental data to this form are shown in Fig. 16. It is interesting that for 30-at. % Fe alloys very good fits are obtained to the highest measured temperatures. This is in contrast to results of fits to Gaunt's theory for activated rotations of single-domain particles in that better fits for low Fe concentration alloys were obtained in that case. This might indicate that in the $x=30$ alloys the spin-reversal mechanism is dominated more by wall diffusion of nucleation processes and in the alloys containing less Fe coherent rotation processes might dominate. ac susceptibility on the $x=30$ alloys suggests magnetic ground states which are different from other alloys of the series. This could be due to an increasing heterogeneity in these samples, caused perhaps by the increasing presence of chemical short-range order. The relatively large coercive fields observed in the $x=30$ alloys would be consistent with this because of increased fluctuations expected in "multiphase" materials.

VI. SUMMARY AND CONCLUSIONS

The Gd glasses containing Fe are apparently simple ferrimagnets with Fe moments opposing the Gd spins as expected. The $(Gd_{80}Ga_{20})_{90}B_{10}$ glass shows a low-temperature hysteretic phase which disappears when Fe is added at the level of 10% or 20%. Also, the Fe-free Gd glass appears to have a relatively high measured anisotropy. These data were interpreted in terms of a system with competing ferromagnetic and spin-glass order, so that the low-temperature falloff of χ_{ac} corresponds to a ferromagnetic–spin-glass transition. The apparent high anisotropy of $(Gd_{80}Ga_{20})_{90}B_{10}$ probably results from some admixture of antiferromagnetic coupling in the overall exchange distribution curve. As Fe is added, the average (ferromagnetic) exchange becomes stronger; one moves away from the presumed multicritical point and the anisotropy weakens.

The alloys containing the anisotropic rare earths terbium and erbium are more complex. None of these alloys approached saturation in high magnetic fields and coercive fields developed at low temperatures. It is interesting that corresponding Tb and Er alloys have qualitatively quite similar properties as evidenced by ac susceptibility and the thermal variation of H_c. The data seem to sug-

gest the possibility that $(Tb_{80}Ga_{20})_{90}B_{10}$ is a loosely interacting system of single-domain particles such as that discussed by Stoner and Wohlfarth.[34] As Fe is added to Tb alloys, discontinuities appear in the initial magnetization as well as the major loops. This might be viewed as evidence suggesting the presence of microdomains as predicted by Chi and Alben[12] or Callen *et al.*[11] However, as Fe is added the reduced remanence increases, suggesting increased interactions. Within the framework of the model of Callen *et al.* the coercive force should decrease, but H_c is also observed to increase as Fe is added. ac susceptibility data on the $x=30$ alloys suggest an increased heterogeneity in these materials. The observed increase of H_c in these alloys seems to be consistent with the theory of Paul[46] as with other alloys. However, the choice of parameters used to calculate $H_c(0)$, although not *arbitrary,* seems somewhat uncertain and microscopic information would be useful.

Although alloys with $x<30$ seem to have a temperature dependence of H_c which is compatible with activation of coherent rotation processes as discussed by Gaunt,[51] the $x=30$ alloys exhibit behavior compatible with activated domain-wall diffusion or nucleation processes as discussed by Egami.[52] Oesterreicher *et al.*[55] have found the form of Eq. (16) to fit well to results on disordered $TbFe_{0.5}Al_{1.5}$ and amorphous $Tb_{0.12}Fe_{0.88}$. The values of V_T obtained are reasonably close to the values reported here for the $x=30$ alloys.

The law of approach to saturation gave results that fit fairly well even though the magnetization curves were far from technical saturation (spin-aligned state). Values of spontaneous magnetization, even though the true ground states of the anisotropic glasses are speromagnetic, are about that expected for a hemisphere of spins ($\frac{1}{2}gJ$/spin). This suggests that most spins in moderate fields spin flop to the upper hemisphere, at which point further alignment becomes more difficult as spins rotate against the forces of anisotropy.

In conclusion, it is seen that the $x=30$ glasses show a character different from that of glasses with $x=0$, 10, and 20. Domain-wall motion or nucleation processes appear to dominate magnetization reversal for $x=30$, while for $x=0$, 10, and 20 a greater tendency for magnetization reversal through coherent rotation processes is seen. The magnetic hardness in these materials is supportive of the model of Paul for heterogeneous magnetic systems. Evidence for this support is the increased magnetic hardness in $x=30$ glasses which show greatly broadened and weakened ac susceptibility peaks and the development of a second broad peak (indicative of increased heterogeneity). It would be interesting to investigate the possibility that as Fe is added, microdomains become larger in volume. This might explain coherent rotation processes at low Fe content since a thermally activated rotation on relatively few spins may easily occur. As the Fe content increases, the microdomain size could increase to a critical value where the energetics of spin rotation favor the nucleation of reverse domains or domain-wall—motion processes.

ACKNOWLEDGMENTS

We thank Mr. J. Nabity for preparing many of our amorphous alloys, Dr. M. J. O'Shea and Dr. G. Hadjipanayis for assistance and helpful discussions, and Dr. Z. D. Chen for help with the ac susceptibility measurements. We are most grateful to the National Science Foundation for financial support under Grant No. DMR-81-10520.

*Present address: Ballistic Research Laboratory, Aberdeen Proving Grounds, Aberdeen, MD 21005.

[1]See R. W. Cochrane, R. Harris, and M. J. Zuckermann, Phys. Rep. **48**, 1 (1978).

[2]N. W. Ashcroft and N. D. Mermin, *Solid State Physics* (Holt, Rinehart, and Winston, New York, 1976).

[3]E. Borchi and S. DeGennaro, J. Phys. F **11**, L47 (1981).

[4]A. Friederich, B. Boucher, and A. Fert, Solid State Commun. **30**, 443 (1979).

[5]K. H. J. Buschow and W. W. Van Den Hoogenhof, J. Magn. Magn. Mater. **12**, 123 (1979).

[6]J. J. Croat, A. R. Charplyuy, and J. F. Herbst, Appl. Phys. Lett. **37**, 962 (1980).

[7]H. Harris, M. Plischke, and M. J. Zuckermann, Phys. Rev. Lett. **31**, 160 (1973).

[8]C. Jayaprakash and S. Kirkpatrick, Phys. Rev. B **21**, 4072 (1980).

[9]M. C. Chi and T. Egami, J. Appl. Phys. **50**, 165 (1979).

[10]R. Harris, J. Phys. F **10**, 2545 (1980).

[11]E. Callen, Y. J. Liu, and J. R. Cullen, Phys. Rev. B **16**, 263 (1977).

[12]M. C. Chi and R. Alben, *Magnetism and Magnetic Materials—1976 (Joint MMM-Intermag Conference, Pittsburgh),* Partial Proceedings of the First Joint MMM-Intermag Conference, edited by J. J. Becker and G. H. Lander (AIP, New York, 1976), p. 316.

[13]R. Alben, J. J. Becker, and M. C. Chi, J. Appl. Phys. **49**, 1653 (1978).

[14]K. J. Strnat, IEEE Trans. Magn. MAG-**6**, 511 (1970).

[15]H. Oesterreicher, Solid State Commun. **14**, 571 (1974).

[16]M. G. Benz and D. L. Martin, J. Appl. Phys. **43**, 4733 (1972).

[17]R. W. Lee, IEEE Trans. Magn. MAG-**15**, 1762 (1979).

[18]R. J. J. Martis, IEEE Trans. Magn. MAG-**15**, 1760 (1979).

[19]D. I. Paul, *Magnetism and Magnetic Materials—1975 (Philadelphia),* Proceedings of the 21st Annual Conference on Magnetism and Magnetic Materials, edited by J. J. Becker, G. H. Lander, and J. J. Rhyne (AIP, New York, 1976), p. 545.

[20]H. Oesterreicher, Appl. Phys. **15**, 341 (1978).

[21]S. G. Cornelison, D. J. Sellmyer, and G. Hadjipanayis, J. Appl. Phys. **52**, 1823 (1981).

[22]S. G. Cornelison, D. J. Sellmyer, J. G. Zhao, and Z. D. Chen, J. Appl. Phys. **53**, 2330 (1982).

[23]F. R. Szofran, W. L. Burmester, D. J. Sellmyer, and L. G. Rubin, Rev. Sci. Instrum. **46**, 1186 (1975).

[24]J. A. Gerber, W. L. Burmester, and D. J. Sellmyer, Rev. Sci. Instrum. **53**, 691 (1982).

[25]S. Chikazumi, *Physics of Magnetism* (Wiley, New York, 1964).

[26]This value is for uniaxial anisotropy. See. H. Zijlstra, *Experimental Methods in Magnetism* (Wiley, New York, 1967), Vol. 2, p. 183.

[27]B. D. Cullity, *Introduction to Magnetic Materials* (Addison-Wesley, Reading, Massachusetts, 1972), p. 317.
[28]H. Kronmüller, IEEE Trans. Magn. MAG-**15**, 1218 (1979).
[29]See. G. Hadjipanayis, D. J. Sellmyer, and B. Brandt, Phys. Rev. B **23**, 3349 (1981).
[30]For a review, see K. V. Rao, Phys. Scr. **25**, 742 (1982).
[31]D. Sherrington and S. Kirkpatrick, Phys. Rev. Lett. **35**, 1792 (1975); Phys. Rev. B **17**, 4394 (1978); see also M. Gabay and G. Toulouse, Phys. Rev. Lett. **47**, 201 (1981).
[32]D. J. Sellmyer and M. J. O'Shea, J. Less-Comm. Met. **94**, 59 (1983).
[33]R. A. Pelcovits, Phys. Rev. **19**, 465 (1979).
[34]E. C. Stoner and E. P. Wohlfarth, Philos. Trans. R. Soc. London, Ser. A **240**, 599 (1948).
[35]P. Rhodes, Proc. Leeds Philos. Lit. Soc. Sci. Sect. **5**, 116 (1948).
[36]A. R. Bishop and W. F. Lewis, J. Phys. C **12**, 3811 (1979).
[37]J. D. Patterson, G. R. Gruzalski, and D. J. Sellmyer, Phys. Rev. B **18**, 1377 (1978).
[38]This is an approximation to results of Ref. 11; see R. Ferrer, R. Harris, S. H. Sung, and M. J. Zuckermann, J. Phys. (Paris) Colloq. **40**, C5-50 (1979); A. K. Bhattacharjee and D. Coqblin, *ibid.* **40**, C5-246 (1979).
[39]J. J. Rhyne, J. H. Schelleng, and N. C. Koon, Phys. Rev. B **10**, 4672 (1974).
[40]R. Tournier and Y. Ishikawa, C. R. Acad. Sci. **259**, 3967 (1964).
[41]T. H. Tsai and D. J. Sellmyer, Phys. Rev. B **20**, 4577 (1979); J. Appl. Phys. **49**, 1507 (1978).
[42]H. Oesterreicher, Appl. Phys. **15**, 341 (1978).
[43]D. I. Paul, in *Amorphous Magnetism II,* edited by H. Levy and R. Hasegawa (Plenum, New York, 1977), p. 403.
[44]J. Chappert, R. Arrese-Buggiano, and J. M. D. Coey, J. Magn. Magn. Mater. **1**, 175 (1978).
[45]S. G. Cornelison, G. Hadjipahayis, and D. J. Sellmyer, J. Non-Cryst. Solids **40**, 429 (1980).
[46]D. I. Paul, J. Appl. Phys. **53**, 1649 (1982); *ibid.* **53**, 2362 (1982).
[47]C. P. Bean and J. D. Livingston, J. Appl. Phys. **30**, 2105 (1959).
[48]P. Gaunt, Philos. Mag. **17**, 263 (1968).
[49]I. Joffa, J. Phys. C **2**, 1537 (1969).
[50]J. Mizra, H. Figiel, and K. Krop, Acta Phys. Pol. **39**, 71 (1971).
[51]P. Gaunt, Phys. Rev. B **19**, 521 (1979).
[52]T. Egami, Phys. Status Solidi A **20**, 157 (1973); **57**, 211 (1973).
[53]This value was obtained by assuming a particle relaxation of time of 10^2 sec, assuming the reversal process is coherent rotation. At 300 K this would imply a 40-Å radius for an hcp cobalt particle. See Ref. 47 for complete details.
[54]H. Oesterreicher, F. T. Parker, and M. Misroch, Phys. Rev. B **18**, 480 (1978).
[55]H. Oesterreicher, F. T. Parker, and M. Misroch, J. Magn. Magn. Mater. **15** 1485 (1980).